SOUTHERN JOURNAL OF SCIENCES

ESTABLISHED IN 1993

Original research paper

STATISTICAL VALIDATION OF TRIPLE COLOCALIZATION ANALYSIS

BUONFIGLI Julio[1*]; QUINTERO Cristian[2,3]; SÁNCHEZ Diego[1]; LEIVA Natalia[4,5]; DAMIANI Maria Teresa[1]

[1]Universidad Nacional de Cuyo, Facultad de Medicina, Laboratorio de Fagocitosis y Transporte intracelular, IMBECU-CONICET, Mendoza, Argentina.

[2]Laboratorio de Biología Molecular y Celular. Universidad Juan Agustín Maza, Mendoza, Argentina.

[3]Facultad de Ciencias Médicas, Universidad de Mendoza, Mendoza, Argentina.

[4]CONICET, Facultad de Ciencias Médicas, Universidad Nacional de Cuyo, M5500 Mendoza, Argentina.

[5]Facultad de Ciencias Exactas y Naturales, Universidad Nacional de Cuyo, M5500 Mendoza, Argentina.

** Corresponding author*
e-mail: juliobuonfigli@yahoo.com.ar

Received 30 July 2023; received in revised form 07 December 2023; accepted 15 December 2023

ABSTRACT

Background: in the last decades, colocalization analysis of fluorescently tagged biomolecules has proven to be a powerful approach to studying functional relationships between these biomolecules. However, in many cases, to give this analysis a biological meaning, colocalization coefficients must be tested statistically, comparing them with the colocalization expected by chance. **Aim:** It addressed the statistical significance of triple colocalization to distinguish real triple colocalization and classify different triple signal scenarios. **Methods:** we use biological and generated images of triple signal scenarios to contrast seven independent statistical facts with independent statistical tests. Three of these tests correspond to pairwise relationships (double scrambling tests), and the others correspond to triple relationships: single scrambling tests (red, green, and blue scrambling) and the triple scrambling test. The analysis and methodology proposed can be reproduced using the application developed in our laboratory. **Results**: In the study approach, we found true triple relationships ignored by using traditional methods of computing the statistical significance, while we could reinterpret cases of not significant triple colocalization wrongly considered as significant by traditional methods. **Discussion:** single scrambling tests can reveal significant triple colocalization for low levels of triple co-occurrence, even when all pairwise relationships were exclusion relationships. Moreover, on the other hand, single scrambling tests can reveal the absence of a significant triple colocalization for high levels of triple co-occurrence, even when all pairwise relationships were significant colocalization. **Conclusion:** all scrambling tests are useful to classify a specific scenario of a triple relationship. Dynamics like mitosis can be distinguished into their phases by triple signal relationships using these 7 independent statistical tests.

Keywords: *Scrambling, overlapping, significance, correlation, triple*.

1. INTRODUCTION:

Colocalization in fluorescence images is one of the most commonly used approaches to study functional interactions between biomolecules. Using fluorescence microscopy techniques, the spatial distribution of two biomolecules is recorded on independent images. Then, the spatial overlapping of the signal of both fluorophores is quantified as a colocalization coefficient (Bolte & Cordelieres, 2006; Dunn, Kamocka, & McDonald, 2011; Oheim & Li, 2007; Zinchuk & Zinchuk, 2008). Unfortunately, colocalization coefficients use fluorescent light signals as inputs, and fluorescence intensity is a non-reproducible parameter. Fluorescence intensity is sensitive to many variables related to the setting of the microscope, fluorophores, and experimental conditions, including variables that are not fully manageable by users, such as the efficiency of the optical coupling, cleanness of optics, environmental perturbations (vibrations and electromagnetic fields), output power and output instability of laser in confocal microscopy, to name a few (Pawley, 2000). Small changes in such variables can make colocalization coefficients yield very different results. Thus, colocalization coefficients cannot be linked to biophysical variables. Statistical analysis gives a probabilistic approach, improving the biological interpretation of colocalization analysis (French, Mills, Swarup, Bennett, & Pridmore, 2008; Lachmanovich *et al*., 2003; Mcdonald & Dunn, 2013). This analysis determines if there exists 'significant colocalization' (SC), which indicates biomolecules tend to be close to each other, 'not significant colocalization' (NS), which means that biomolecules only meet each other by chance, or 'significant exclusion' (SE) which means that biomolecules avoid each other. Then, depending on the resolution of images, this tendency to be close (SC) can be associated with biophysical variables ranging from physicochemical similarities and co-compartmentalization to direct interactions (Jeremy Adler & Parmryd, 2010; French *et al*., 2008; Lagache, Sauvonnet, Danglot, & Olivo-Marin, 2015; Malkusch *et al*., 2012)

Costes et al. developed one of the most used approaches to address statistical significance for two-channel colocalization analysis (Costes *et al*., 2004). They proposed to compare actual colocalization coefficients with the one obtained when pixels (or blocks of pixels) of one or both channels are randomly rearranged, an approach known as 'scrambling'. This coefficient, measured using scrambled images, serves as a virtual control that simulates random colocalization. The scrambling procedure is repeated as many times as necessary to validate the existence or absence of a significant difference with the actual coefficient. Other approaches can be cited (Fay, Taneja, Shenoy, Lifshitz, & Singer, 1997; Li *et al*., 2004; Lifshitz, 1998; Mcdonald & Dunn, 2013; Ramírez, García, Rojas, Couve, & Härtel, 2010; Van Steensel *et al*., 1995), but all of them are strictly focused on pairwise colocalization analysis, and although, some of these approaches can be adapted for three channels, this matter is loosely addressed in the existent bibliography. Triple colocalization cannot be inferred from the analysis of pairwise relationships. A triple grouping behaves differently from pairwise groupings (Fletcher, Scriven, Schulson, & Moore, 2010). Thus, considering any three channels analysis with red (R), green (G) and blue (B) signals, a triple colocalization (RGB) may exist in the absence of significant pairwise colocalization (RG; RB; GB), and conversely, even when all pairwise colocalizations (RG; RB; GB) were significant, this does not necessarily imply the existence of a significant triple colocalization (RGB). Some authors have addressed the issue of triple colocalization (Fletcher *et al*., 2010; Goucher, Wincovitch, Garfield, Carbone, & Malik, 2005; Wörz *et al*., 2010) but Fletcher *et al* are the only authors who have performed a statistical significance on triple colocalization analysis (Fletcher *et al*., 2010). They proposed a statistical test of triple colocalization in which random triple colocalization is simulated by scrambling all channels to simulate random colocalization. Although this test yields valuable information for colocalization analysis, it fails when it is isolated to judge a triple colocalization.

This work explores the scope of triple colocalization analysis from a statistical perspective. We use biological and generated images to show the importance of triple colocalization analysis as an independent subject not inferrable from pairwise relationships. In this respect, we follow a methodology based on co-occurrence analysis using MOC (Manders overlap coefficient). We contrast seven independent statistical facts with seven different statistical tests. Three of these tests correspond to pairwise relationships (double scrambling tests), and the others

correspond to triple relationships: single scrambling tests (red, green, and blue scrambling) and the triple scrambling test. The study shows how all these tests are useful to understand pairwise and triple colocalization. The proposed analysis and methodology can be reproduced using the application at https://gitlab.com/juliobuonfigli/tcss

2. MATERIALS AND METHODS

2.1. Materials

Both the generation of simulated colocalization images and manipulation (crops and rotations) of the microscopy image were performed using ImageJ 1.52p. All colocalization and statistical analysis were performed by an ImageJ application available at https://gitlab.com/juliobuonfigli/tcss. The script mentioned above also details of how to use it. Histograms of Figure 1 were made using the stats program SPSS Statistics 24.0.0.

2.1.1 List of software used in script writing:

- Notepad;
- ImageJ;

2.2. Methods

Biological and generated images were used to recreate different triple colocalization scenarios and test our approach.

2.2.1 Biological and generated images

It was generate 2 and 3 channels binary images with 20 (Figure 1Ai and 1Bi), 35 (Figure 1Ci), and 10 (Figure 1Ciii) round objects of 15 (Figure 1Ai, 1Bi, and 1Ci) and 30 (Figure 1Ciii) pixels diameter on each channel, in a total area of 200x200 pixels. To generate random triple overlapping, the center of all blue objects (Figure 1Bi) and all overlapped pairs of objects (Figure 1Ciii) were randomly positioned using the random function of the ImageJ. After 100 randomizations for each case, the merge with the median MOC_{RGB} was selected in both cases. Scrambling examples (Figure 1Aii, 1Aiv, 1Avi, 1Bii, 1Bv, 1Bvii, and 1Bix) were generated by rendering a series of rearranged actual images of 15 pixels block (Figure 3B) and merging with actual or other scrambled images.

A single image with seven selected samples of the mitosis phases was downloaded from https://wellcomecollection.org/works/r8ppshar. The original image (Figure 3A) shows all mitosis phases (interphase, prophase, prometaphase, metaphase, early anaphase, anaphase, and telophase) in which kinetochores are labeled in red, tubulin in green, and DNA in blue, in a 3000x2250 pixels JPG image. Each phase was cropped and rotated to be analyzed separately. No treatments or filters were applied to the full-size image and crops.

2.2.2 Coefficients

For pairwise relationships, the Manders overlap coefficient (MOC) is given by:

$$MOC_{RG}=\Sigma(R_i*G_i)/(\Sigma R_i^2*\Sigma G_i^2)^{1/2} \quad \text{(Eq. 1)}$$

Where R_i is the intensity of the i^{th} pixel in the red channel, and G_i is the intensity of the i^{th} pixel in the green channel. This coefficient ranges from 0 to 1 and measures the proportion of colocalized signals over the total amount of both signals (MANDERS, VERBEEK, & ATEN, 1993). To measure triple overlapping, we add a third series to the equation:

$$MOC_{RGB}=\Sigma(R_i*G_i*B_i)/(\Sigma R_i^3*\Sigma G_i^3*\Sigma B_i^3)^{1/3} \quad \text{(Eq. 2)}$$

where B_i is the intensity of the i^{th} pixel in the blue channel. MOC_{RGB} ranges from 0 to 1 and measures the proportion of colocalized signals over the total amount of signals. Manders colocalization coefficient (MCC) (MANDERS *et al.*, 1993) is given by:

$$MCC_{RG}=\Sigma(R_{iG})/(\Sigma R_i) \quad \text{(Eq. 3)}$$

$$MCC_{R\text{-}GB}=\Sigma(R_{iGB})/(\Sigma R_i) \quad \text{(Eq. 4)}$$

Where R_{iG} is the intensity of the i^{th} pixel in the red channel that colocalizes with a green pixel above the intensity threshold, and R_{iGB} is the intensity of the i^{th} pixel in the red channel that

colocalizes with a green and blue pixel above their respective intensity thresholds. MCC_{RG} measures the proportion of red signal that colocalizes with green signal, and $MCC_{R\text{-}GB}$ measures the proportion of red signal that colocalizes with green and blue signals. With three channels, there are 9 MCC coefficients with subscripts: RG, GR, RB, BR, GB, and BG for pairwise relationships, and R-GB, G-RB and B-RG for triple colocalization.

2.2.3 Running the plugin

The script runs as a plugin of the opensource program ImageJ, available at https://imagej.net/ij/. The script is available at https://gitlab.com/juliobuonfigli/tcss. To run the script:

1) Install the plugin by saving this file in the ImageJ\plugins\Macros folder and restart ImageJ

Then click in plugins->macros->install and search this file in the ImageJ\plugins\Macros folder.

2) Open the three channels to use and generate the mask if necessary

The mask is a binary image of the same dimensions as the channels, with intensities of 255 inside and 0 outside the ROI

3) Run the macro by clicking plugins->macros->TCSS or pressing the 'c' key

4) Load the channels and the mask

5) Select an approach to set thresholds as:

- The average intensity value inside the ROI plus x standard deviations settled by the user from -2 to 2

- A percentage of pixels higher than zero inside the ROI (from 0 to 100)

- An intensity value from 0 to 255

6) Set the intensity threshold values for each channel according to the approach selected

7) Select the scrambling approach:

- Coordinates: randomly changes the origin of coordinates of actual channels (Lifshitz approach)

- Pixels: randomly relocates all pixels (Costes approach)

- Blocks of pixels: randomly relocates blocks of pixels (Costes approach)

If 'Blocks of pixels' is selected the, the block size must be set as an area of pixels

Block of pixels approach will not run with a mask-loaded

8) Set the hypothesis test:

- T-test approach

- Non-parametric approach: the ratio of the amount of random coefficients higher than the actual value and the totality of random coefficients measured

9) Set the number of generated images: the number of times actual channels will scramble to generate the random overlapping distribution. set it to zero to calculate just coefficients

10) Set the significance level (0.01 or 0.05): the cut-off point of p-values to consider the test SC, SE or NS

11) Set the random seed: a positive integer that points to the beginning of the series of pseudorandom numbers. Please set it to zero for a random beginning

RESULTS:

A table shows the coefficient (MOC or MCC) for each relationship;

The average of random coefficients (random); the significance result (significance); and the p-value.

The least related channel (LRC) is indicated with an arrow ('<') in the first column of triple colocalization relationships

Graphical results are summarized in a stack that displays examples of scrambled channels and the merge of the thresholded channels

2.2.4 Data processing

Statistical significances of analysis performed in Fig. 1 were made by repeating the scrambling procedure (Figure 3B) 1000 times and then performing a one-tailed hypothesis test with an error tolerance of 5%. The block size was settled according to the diameter of the objects. For microscopy images, due to the difficulty of object segmentation and thus setting the proper block size and avoiding altering the autocorrelation of each channel (Bolte & Cordelieres, 2006), we followed the Lifshitz

approach (Lifshitz, 1998). Scrambled images were generated by randomly changing the coordinates of the origin of actual channels (Figure 3C). To find p-values, a non-parametric approach was used: the ratio of the number of random coefficients higher than the actual MOC value and the totality of random coefficients measured. To avoid altering autocorrelation by the scrambling process (Lifshitz approach), squared regions of interest (ROIs) were used. ROIs were set as the biggest square that can be fitted inside cell edges (Figure 2B). Experiments of Fig. 1 were done using both randomization approaches and yielded the same significant results. For microscopy images, signal thresholds were set at the average intensity value of the signal inside the ROI.

2.2.5 Source code (tcss / TCSS.txt)

```
/*
*Triple Colocalization Statistical
Significance (TCSS)
*Author: Julio Federico Buonfigli
*e-mail: juliobuonfigli@yahoo.com.ar
Version 6.01
This code is licensed under CC BY 4.0
(https://creativecommons.org/licenses/
by /4.0/).
You are free to share and adapt the
code, but you must provide appropriate
credit to the original author.
DOI:
10.48141/SBJCHEM.v31.n36.2023_BUONFIGL
I_pg s_45_62.pdf
*/
macro "TCSS [c]" {

BATCH=false;
if(BATCH) arg1=getArgument();
MCC=false;
//MCC=true;

//FUNCTIONS

function TheLeast(vec, c0, c1, c2)
//Finds the least related channel
using p-vaules
    {
    v=vec; m=c0;
    if(c1<m) m=c1;
    if(c2<m) m=c2;
    if(m==c0)
        v[2]=vec[2]+"<";
    if(m==c1)
        v[1]=vec[1]+"<";
    if(m==c2)
        v[0]=vec[0]+"<";
    return v;
    }

//'A Fairly Accurate Approximation to
the Area Under Normal Curve', AMIT
CHOUDHURY AND PARAMITA ROY, 2009
function Pvalue(x)  //calculates p-
value
    {
    if(x<0) {indi=1; x=(-1)*x; }
    else indi=0;

    if(x<=2.0885 && x>0){
    t=0.5 + (1/sqrt(2*PI))*exp(-pow(x,
2)/2)*((654729075*x + 45945900*pow(x,
3)
    + 6486480*pow(x, 5) +
154440*pow(x, 7) + 4785*pow(x,
9))/(654729075
    - 172297125*pow(x, 2) +
20270250*pow(x, 4) - 1351350*pow(x, 6)
+ 51975
    *pow(x, 8) - 945*pow(x, 10)));}

    if(x<1.8735 && x>0) y=t;

    if(x>=1.8735 && x<=2.0885)
    y = t - 0.00007237 + 0.0000768*x -
0.00002041*pow(x, 2);

    if(x>2.0885 && x<=5.75){
    t=1 - (1/(2*sqrt(2*PI)))*exp(-
pow(x, 2)/2)*((5790*x + 5280*pow(x, 3)
+ 1176*
    pow(x, 5) + 88*pow(x, 7) +
2*pow(x, 9))/(945 + 4725*pow(x, 2) +
3150*
    pow(x, 4) + 630*pow(x, 6) +
45*pow(x, 8) + pow(x, 10)));}

    if(x>2.0885 && x<2.43)
    y = t - 0.00004861 + 0.00004021*x
- 0.00000833*pow(x, 2);

    if(x>2.43 && x<=5.75) y=t;

    if(x>5.75) y=1;

    if(indi==0) z=1-y;
    else
        {
        if(x==0) z=0.5;
        else z=y;
        }
    return(z)
    }

function Renderize(vec, masc, img)
//Transforms a vector to an image
    {
    selectWindow(img);
    w=getWidth; h=getHeight;
    j=0; i=0;
    for(y=0; y<h; y++)
        {
        for(x=0; x<w; x++)
```

```
            {
            if(masc[i]==255)
                {
                setPixel(x, y,
vec[j]);
                j++;
                }
            i++;
            }
        }
    }

function Pthreshold(canal, unos, prop)
//Calculates the threshold to keep a
specific percentage of signal inside
the ROI
    {
    umbral=256;
    vec=newArray(umbral);
    for(j=0; j<umbral; j++)
        vec[j]=0;
    for(i=0; i<unos; i++)
        vec[canal[i]]=vec[canal[i]]+1;
    cuenta=0;
    do  {
        umbral--;
        cuenta=cuenta+vec[umbral];
        } while(cuenta <
unos*(prop/100))
    return umbral;
    }

function Vectorize(image, w, h)
//Vectorize an image
    {
    selectWindow(image);
    vec=newArray(w*h);
    i=0;
    for (y=0; y<h; y++)
        {
        for (x=0; x<w; x++)
            {
            vec[i] = getPixel(x,y);
            i++;
            }
        }
    return vec;
    }

function PixelRand(vector) //Shuffles
an array
    {
    ones=vector.length;
    u=newArray(ones+1);
    for(i=0; i<ones; i++)
        u[i]=true;
    rd=newArray(ones);
    i=0;
    while(i<ones)
        {
        e=round(random*ones);
        if(u[e]==true)
            {
            rd[i]=vector[e];
            u[e]=false;
            i++;
            }
        }
    return rd;
    }

function CoordRand(vec, ones) //shifts
the beginning of a vector
    {
    j=round((ones-1)*random);
    v=newArray(ones);
    for(i=0; i<ones; i++)
        {
        v[i]=vec[j];
        j++;
        if(j>ones-1) j=0;
        }
    return v;
    }

function BlockRand(vec, w, h, r)
//generates the block scrambling of a
vector
    {
    X=w/r; Y=h/r;
    pos=newArray(X*Y);
    i=0;
    for(y=0; y<Y; y++)
        {
        for(x=0; x<X; x++)
            {
            pos[i]=w*y*r+x*r;
            i++;
            }
        }
    ran=newArray(X*Y);
    ran=PixelRand(pos);
    v=newArray(w*h);
    for(i=0; i<ran.length; i++)
        {
        j=ran[i]; k=pos[i];
        for(y=0; y<r; y++)
            {
            for(x=0; x<r; x++)
                {
                v[k]=vec[j];
                j++; k++;
                }
            j=j+w-r;
            k=k+w-r;
            }
        }
    return v;
    }

function Threshold(vec, um, ones)
//Thresholds an array
    {
    ar=newArray(ones);
    for(i=0; i<ones; i++)
        {
        if(vec[i]>=um)
            ar[i]=vec[i];
```

```
            else
            ar[i]=0;
        }
    return ar;
    }

function Sig(rat, lev) //Evaluates the
significance
    {
    if(rat<lev)
        sig="SC";
        else
        {
        if(rat>1-lev)
            sig="SE";
            else
            sig="NS";
        }
    return sig;
    }

function Tcoloc(c1, c2, c3, mcc)
//calculates MOC or MCC coefficient
for three channels
    {
    l=c1.length;
    coef=0; denC1=0; denC2=0; denC3=0;
num=0;
    if(mcc)
        {
        for(i=0; i<l; i++)
            {
            if(c2[i]>0 && c3[i]>0)
num=num+c1[i];
            denC1=denC1+c1[i];
            }
        coef=num/denC1;
        }
    else
        {
        for(i=0; i<l; i++)
            {

denC1=denC1+c1[i]*c1[i]*c1[i];

denC2=denC2+c2[i]*c2[i]*c2[i];

denC3=denC3+c3[i]*c3[i]*c3[i];
            num=num+c1[i]*c2[i]*c3[i];
            }

coef=num/cbrt(denC1*denC2*denC3);
        }
    return coef;
    }

function Dcoloc(c1, c2, mcc)
//calculates MOC or MCC coefficient
for two channels
    {
    l=c1.length;
    coef=0; denC1=0; denC2=0; num=0;
    if(mcc)
        {
        for(i=0; i<l; i++)
            {
            if(c2[i]>0) num=num+c1[i];
            denC1=denC1+c1[i];
            }
        coef=num/denC1;
        }
    else
        {
        for(i=0; i<l; i++)
            {
            denC1=denC1+c1[i]*c1[i];
            denC2=denC2+c2[i]*c2[i];
            num=num+c1[i]*c2[i];
            }
        coef=num/sqrt(denC1*denC2);
        }
    return coef;
    }

function Msd(v) //calculates the mean
and standard deviation of an array
    {
    l=v.length;
    pd=newArray(2);
    pd[0]=0;
    for(i=0; i<l; i++)
        pd[0]=pd[0]+v[i];
    pd[0]=pd[0]/l;
    pd[1]=0;
    for(j=0; j<l; j++)
        pd[1]=pd[1]+(v[j]-
pd[0])*(v[j]-pd[0]);
    pd[1]=sqrt(pd[1]/(l-1));
    return pd;
    }

function Cut(vec, mas, an, al, ones)
    {
      j=0;
      ar=newArray(ones);
      for(i=0; i<an*al; i++)
        {
        if(mas[i]==255) {
            ar[j]=vec[i];
            j++;
            }
        }
    return ar;
    }

function Count(m) //counts non-zero
pixels
    {
    cont=0;
    for(i=0; i<m.length; i++) {
        if(m[i]>0)
            cont++; }
    return cont;
    }

function cbrt(w) //calculates the
cubic root
    {
```

```
    x=w; y=1;  e=0.0001;
    while(x-y>e)
        {
        x=(2*x+y)/3;
        y=w/(x*x);
        }
    return x;
    }

//DIALOG WINDOW
img=getList("image.titles");
if(img.length==0) exit("At least 2
images opened");
img2=newArray(nImages+1);
img2[0]="none";
for(i=1; i<nImages+1; i++)
    img2[i]=img[i-1];

  TNUM=newArray(3);
if(BATCH==false)
  {
  Dialog.create("TCSS");
  Dialog.addChoice("Red", img);
  Dialog.addChoice("Green", img);
  Dialog.addChoice("Blue", img2);
  Dialog.addChoice("Mask", img2);
  Dialog.addChoice("Thresholding
approach", newArray("Mean+sd (-2/2)",
"Porcentual (0/100)", "Numeric
(0/255)"));
  Dialog.addNumber("Red threshold",
0);
  Dialog.addNumber("Green threshold",
0);
  Dialog.addNumber("Blue threshold",
0);
  Dialog.addChoice("Scrambling
approach", newArray("Coordinates",
"Blocks of Pixels", "Pixels"));
  Dialog.addNumber("Block area
(pixels)", 225);
  Dialog.addChoice("Hypothesis test",
newArray("Non-parametric", "T-test"));
  Dialog.addNumber("Number of
generated images", 30);
  Dialog.addChoice("Significance
level", newArray(0.05, 0.01));
  Dialog.addNumber("Random seed
(positive integer)", 1);

  Dialog.show();
  RED=Dialog.getChoice();
  GREEN=Dialog.getChoice();
  BLUE=Dialog.getChoice();
  PMASK=Dialog.getChoice();
  STCRITERION=Dialog.getChoice();
  TNUM[0]=Dialog.getNumber();
  TNUM[1]=Dialog.getNumber();
  TNUM[2]=Dialog.getNumber();
  RANDCRITERION=Dialog.getChoice();
  BAREA=Dialog.getNumber();
  HTAPPOROACH=Dialog.getChoice();
  GIMAGES=Dialog.getNumber();
  SLEVEL=Dialog.getChoice();
  SEED=Dialog.getNumber();
  }
else
  {
  //BATCH SETTINGS
  RED=img[2];
  GREEN=img[1];
  BLUE=img[0];
  PMASK="none";//img[3];
  STCRITERION="Mean+sd (-5/5)";
  TNUM[0]=0;
  TNUM[1]=0;
  TNUM[2]=0;
  RANDCRITERION="Blocks of Pixels";
  BAREA=400;
  HTAPPOROACH="Simple sampling";
  GIMAGES=1000;
  SLEVEL=0.05;
  SEED=1;
  RIBOOLEAN=true;
  }

//GENERAL SETTINGS
if(RANDCRITERION=="Blocks of Pixels"
&& PMASK!="none")
    exit("No masking allowed if
'Blocks of Pixels' randomization
approach is selected");

BAREA=round(sqrt(BAREA));

if(SEED==0) random("seed",
round(random*100000));
else random("seed", SEED);

selectWindow(RED); run("Select None");
run("8-bit");
selectWindow(GREEN); run("Select
None"); run("8-bit");
if(BLUE!="none") {selectWindow(BLUE);
run("Select None"); run("8-bit");}
W = getWidth;
H = getHeight;

if(RANDCRITERION=="Blocks of Pixels")
{ //adjusts the size of the images
according to an integer number of
blocks
    W=W-1; H=H-1;
    do{W++;}while(W%BAREA!=0)
    do{H++;}while(H%BAREA!=0)
    selectWindow(RED); run("Size...",
"width=W height=H depth=1
interpolation=Bilinear");
    selectWindow(GREEN);
run("Size...", "width=W height=H
depth=1 interpolation=Bilinear");
    if(BLUE!="none")
{selectWindow(BLUE); run("Size...",
"width=W height=H depth=1
interpolation=Bilinear");}}

//MASKING
```

```
R1=newArray(W*H); R1=Vectorize(RED, W,
H);
G1=newArray(W*H); G1=Vectorize(GREEN,
W, H);
if(BLUE!="none") {B1=newArray(W*H);
B1=Vectorize(BLUE, W, H);}
M=newArray(W*H); for(i=0; i<W*H; i++)
M[i]=255;
MAREA=W*H;
if(PMASK!="none") {
    selectWindow(PMASK); run("Select
None");
    M=Vectorize(PMASK, W, H);
    MAREA=Count(M);
    R=Cut(R1, M, W, H, MAREA);
    G=Cut(G1, M, W, H, MAREA);
    if(BLUE!="none") B=Cut(B1, M, W,
H, MAREA); }
else { R=R1; G=G1; if(BLUE!="none")
B=B1; }

//SIGNAL THRESHOLD
if(STCRITERION=="Mean+sd (-2/2)") {
    msd=Msd(R);
TNUM[0]=msd[0]+TNUM[0]*msd[1];
    msd=Msd(G);
TNUM[1]=msd[0]+TNUM[1]*msd[1];
    if(BLUE!="none") {msd=Msd(B);
TNUM[2]=msd[0]+TNUM[2]*msd[1]; }}
if(STCRITERION=="Porcentual (0/100)")
{
    TNUM[0]=Pthreshold(R, MAREA,
TNUM[0]);
    TNUM[1]=Pthreshold(G, MAREA,
TNUM[1]);
    if(BLUE!="none")
TNUM[2]=Pthreshold(B, MAREA, TNUM[2]);
}
//print(TNUM[0]+"   "+TNUM[1]+"
"+TNUM[2]);
R=Threshold(R, TNUM[0], MAREA);
G=Threshold(G, TNUM[1], MAREA);
if(BLUE!="none") B=Threshold(B,
TNUM[2], MAREA);

//COEFFICIENTS
RG=Dcoloc(R, G, MCC);
if(BLUE!="none") { RB=Dcoloc(R, B,
MCC); GB=Dcoloc(G, B, MCC);
RGB=Tcoloc(R, G, B, MCC); RGBR=RGB;
if(MCC==true) { RGBG=Tcoloc(G, R, B,
MCC); RGBB=Tcoloc(B, G, R, MCC); }
else { RGBG=RGB; RGBB=RGB; }}

//RANDOM IMAGES AND RANDOM OVERLAPPING
rg=newArray(GIMAGES);
if(BLUE!="none") {
rb=newArray(GIMAGES);
gb=newArray(GIMAGES);
rgb=newArray(GIMAGES);
rgbr=newArray(GIMAGES);
rgbg=newArray(GIMAGES);
rgbb=newArray(GIMAGES);}

for(s=0; s<GIMAGES; s++)
    {
    showStatus(s);
    if(RANDCRITERION=="Blocks of
Pixels") {
        rR=BlockRand(R, W, H, BAREA);
rG=BlockRand(G, W, H, BAREA);
if(BLUE!="none") rB=BlockRand(B, W, H,
BAREA); }
    if(RANDCRITERION=="Pixels") {
        rR=PixelRand(R);
rG=PixelRand(G); if(BLUE!="none")
rB=PixelRand(B); }
    if(RANDCRITERION=="Coordinates") {
        rR=CoordRand(R, MAREA);
rG=CoordRand(G, MAREA);
if(BLUE!="none") rB=CoordRand(B,
MAREA); }
    rg[s]=Dcoloc(rR, rG, MCC);
    if(BLUE!="none") {
rb[s]=Dcoloc(rR, rB, MCC);
    gb[s]=Dcoloc(rG, rB, MCC);
    rgb[s]=Tcoloc(rR, rG, rB, MCC);
    rgbr[s]=Tcoloc(rR, G, B, MCC);
    rgbg[s]=Tcoloc(rG, R, B, MCC);
    rgbb[s]=Tcoloc(rB, R, G, MCC); }
    //if(s==0) print("RG double
scrambling, RG red scrambling, RG
green scrambling, RGB triple
scrambling, RGB red scrambling, RGB
green scrambling, RGB blue
scrambling");
    //print(d2s(rg[s], 6)+",
"+d2s(Dcoloc(rR, G, MCC), 6)+",
"+d2s(Dcoloc(R, rG, MCC), 6)+",
"+d2s(rgb[s], 6)+", "+d2s(rgbr[s],
6)+", "+d2s(rgbg[s], 6)+",
"+d2s(rgbb[s], 6));
    }

//SIGNIFICANCE
pRG=Msd(rg);
if(BLUE!="none") { pRB=Msd(rb);
pGB=Msd(gb);
pRGBR=Msd(rgbr); pRGBG=Msd(rgbg);
pRGBB=Msd(rgbb); pRGB=Msd(rgb);}

if(GIMAGES>1)
    {
    if(HTAPPOROACH=="T-test")
        {
        cRG=Pvalue((RG-
pRG[0])/pRG[1]);
        if(BLUE!="none") {
cRB=Pvalue((RB-pRB[0])/pRB[1]);
cGB=Pvalue((GB-pGB[0])/pGB[1]);
        cRGBR=Pvalue((RGBR-
pRGBR[0])/pRGBR[1]);
cRGBG=Pvalue((RGBG-
pRGBG[0])/pRGBG[1]);
        cRGBB=Pvalue((RGBB-
pRGBB[0])/pRGBB[1]); cRGB=Pvalue((RGB-
pRGB[0])/pRGB[1]); }
        }
```

```
        else
        {
        cRG=0; if(BLUE!="none") {
cRB=0; cGB=0; cRGBR=0; cRGBG=0;
cRGBB=0; cRGB=0; }
        for(i=0; i<GIMAGES; i++)
            {
            if(rg[i]>RG) cRG++;
            if(BLUE!="none") {
if(rb[i]>RB) cRB++;
            if(gb[i]>GB) cGB++;
            if(rgbr[i]>RGBR) cRGBR++;
            if(rgbg[i]>RGBG) cRGBG++;
            if(rgbb[i]>RGBB) cRGBB++;
            if(rgb[i]>RGB) cRGB++;  }
            }
        cRG=cRG/GIMAGES;
        if(BLUE!="none") {
cRB=cRB/GIMAGES; cGB=cGB/GIMAGES;
        cRGBR=cRGBR/GIMAGES;
cRGBG=cRGBG/GIMAGES;
cRGBB=cRGBB/GIMAGES;
cRGB=cRGB/GIMAGES; }
        }
    sRG=Sig(cRG, SLEVEL);
    if(BLUE!="none") { sRB=Sig(cRB,
SLEVEL); sGB=Sig(cGB, SLEVEL);
sRGBR=Sig(cRGBR, SLEVEL);
sRGBG=Sig(cRGBG, SLEVEL);
sRGBB=Sig(cRGBB, SLEVEL);
sRGB=Sig(cRGB, SLEVEL); }
    cRG=d2s(cRG, 7);
    if(BLUE!="none") { cRB=d2s(cRB,
7); cGB=d2s(cGB, 7); cRGBR=d2s(cRGBR,
7); cRGBG=d2s(cRGBG, 7);
cRGBB=d2s(cRGBB, 7); cRGB=d2s(cRGB,
7); }
    }
else
    {
    pRG[0]=" *****"; if(BLUE!="none")
{ pRB[0]=" *****"; pGB[0]=" *****";
pRGB[0]=" *****"; pRGBR[0]=" *****";
pRGBG[0]=" *****"; pRGBB[0]=" *****";
}
    sRG=" *****"; if(BLUE!="none") {
sRB=" *****"; sGB=" *****"; sRGB="
*****"; sRGBR=" *****"; sRGBG="
*****"; sRGBB=" *****"; }
    cRG=" *****"; if(BLUE!="none") {
cRB=" *****"; cGB=" *****"; cRGB="
*****"; cRGBR=" *****"; cRGBG="
*****"; cRGBB=" *****"; }
    }

//RESULTS TABLE
if(BATCH==false) {
LEAST=newArray(" Red", " Green", "
Blue");
if(GIMAGES>1 && BLUE!="none")
LEAST=TheLeast(LEAST, cRG, cRB, cGB);
titulo1 = "Results";
titulo2 = "["+titulo1+"]";
  f = titulo2;
if (isOpen(titulo1))
    print(f, "\\Clear");
else
run("Table...", "name="+titulo1+"
width=250 height=600");
print(f, "\\Headings:for\t Overlap\t
random\t  Significance\t  p-value");
print(f, "Double colocalization");
print(f, " RG"+"\t  "+RG+"\t
"+pRG[0]+"\t  "+sRG+"\t  "+cRG);
//poner el coso decimal arriba en el
resultado
if(BLUE!="none") {
print(f, " RB"+"\t  "+RB+"\t
"+pRB[0]+"\t  "+sRB+"\t  "+cRB);
print(f, " GB"+"\t  "+GB+"\t
"+pGB[0]+"\t  "+sGB+"\t  "+cGB);
print(f, "Triple colocalization");
print(f, LEAST[0]+"\t  "+RGBR+"\t
"+pRGBR[0]+"\t  "+sRGBR+"\t  "+cRGBR);
print(f, LEAST[1]+"\t  "+RGBG+"\t
"+pRGBG[0]+"\t  "+sRGBG+"\t  "+cRGBG);
print(f, LEAST[2]+"\t  "+RGBB+"\t
"+pRGBB[0]+"\t  "+sRGBB+"\t  "+cRGBB);
print(f, " Triple"+"\t  "+RGB+"\t
"+pRGB[0]+"\t  "+sRGB+"\t  "+cRGB); }
print(f, ""); }
else {
LEAST=newArray("R", "G", "B");
if(BLUE!="none") LEAST=TheLeast(LEAST,
cRG, cRB, cGB);
print(arg1);
print(RG+","+sRG+","+cRG);
 if(BLUE!="none")
{print(RB+","+sRB+","+cRB);
print(GB+","+sGB+","+cGB);
print(RGBR+","+sRGBR+","+cRGBR+","+LEA
ST[0]);
print(RGBG+","+sRGBG+","+cRGBG+","+LEA
ST[1]);
print(RGBB+","+sRGBB+","+cRGBB+","+LEA
ST[2]);
print(RGB+","+sRGB+","+cRGB); }
print(""); }

//GRAPHICS RESULTS

if(GIMAGES>0)  {
    newImage("stack-RandRed", "8-bit
black", W, H, 1);
    Renderize(rR, M, "stack-RandRed");
run("Red");
    newImage("stack-RandGreen", "8-bit
black", W, H, 1);
    Renderize(rG, M, "stack-
RandGreen");  run("Green");
    if(BLUE!="none") {
    newImage("stack-RandBlue", "8-bit
black", W, H, 1);
    Renderize(rB, M, "stack-
RandBlue"); run("Blue");  }} //end if
newImage("Red", "8-bit black", W, H,
1);  Renderize(R, M, "Red");
```

```
newImage("Green", "8-bit black", W, H, 1);  Renderize(G, M, "Green");
if(BLUE!="none") { newImage("Blue", "8-bit black", W, H, 1);  Renderize(B, M, "Blue");}
if(BLUE!="none") { run("Merge Channels...", "c1=Red c2=Green c3=Blue create"); run("RGB Color"); }
else run("Merge Channels...", "c1=Red c2=Green create"); run("RGB Color");
selectWindow("Composite"); close();
selectWindow("Composite (RGB)");
rename("stack-Composite");
run("Images to Stack", "name=Stack title=stack use");
}//END MACRO
```

3. RESULTS AND DISCUSSION

3.1. Results

The orientation of pixel based colocalization analysis is defined foremost by the election of the colocalization coefficient. Pixel based analysis can be classify in two main categories: co-occurrence and correlation (Aaron, Taylor, & Chew, 2018). The first one describes the degree of spatial overlap between signals and use mainly Manders colocalization coefficient (MCC) and Manders overlap coefficient (MOC) (MANDERS *et al*., 1993). Correlation analysis describes the degree of intensity correlation between the overlapped portion of signals, measured using Pearson and Sperman coefficients (J. Adler, Pagakis, & Parmryd, 2008; Manders, Stap, Brakenhoff, Van Driel, & Aten, 1992). In this work we focus on co-occurrence analysis and use MOC coefficient because of its sensibility and simplicity (each relationship is measured in a single coefficient). Additionally, MOC coefficient can be straightforwardly extended to measure triple overlapping (Eq. 2).

3.1.1 Identifying the channel that least colocalizes with the other two is the key to evaluate triple colocalization

The most used statistical test is the Costes scrambling approach. Figure 1Ai shows a two-channel merge of high overlapping (yellow tones). The merge of the left panel comprises 15 round objects of the red channel (R) and 15 objects of the green channel (G) deliberately centered in coordinates close to the center of objects of R. The scrambling approach consists of randomly rearranging the position of blocks of pixels of both channels and then measuring the overlapping of these channels (Figure 1Aii). This procedure is repeated as many times as necessary to compose a distribution of random overlapping and contrasts the actual overlapping value with the distribution. Significant colocalization (SC) is assumed if the area under the Gaussian distribution is lesser than 5% of the total area to the right of the actual overlapping value; significant exclusion (SE) for an area greater than 95%; and not significant colocalization (NS) otherwise (Figure 1Aiii, v, and vii). A key point to consider in two channel analysis is that the same result is obtained by scrambling R, G or both channels (Figure 1Aii, iv and vi), as shown on the overlapping distributions for each case, all sharing the same mean and kurtosis (Figure 1Aiii, v and vii). Contrastingly, on triple colocalization analysis, the scrambling of each channel generates different overlapping distributions. In Figure 1Bi a third blue channel (B) with 15 objects was added to the merge shown in Figure 1Ai. Objects of B were randomly distributed generating a weak overlapping with isolated R objects (magenta pixels), with isolated G objects (cyan pixels) and with the overlapped R and G signals (white pixels). Pairwise relationships with B, RB and GB are NS (Figure 1Biv). The result of triple colocalization statistical significance depends on which channel is scrambled to compose the random overlapping distribution. Red scrambling generates a triple overlapping distribution far to the left of actual overlapping value (MOC_{RGB}=0.1887), thus this test yield SC (Figure 1Bii and iii). Equivalent distributions are generated by green scrambling and triple scrambling, both resulting in SC (Figure 1Bv, vi, ix and x). Blue scrambling is the only test in which the strong existing colocalization between R and G is conserved. This shifts the distribution to the right, including the actual overlapping value inside the area of NS results (Figure 1Bvii and viii). Regarding in this scenario, randomly arranged blue objects generated triple overlapping triple colocalization should be taken as NS, and blue scrambling is the only test that yields this result. B is the channel that least colocalizes with the other two in pairwise relationships or the least related channel (LRC), formally established as the channel that is not involved in the pairwise relationship with the smallest p-value (Figure 1Biv).

3.1.2 Triple colocalization cannot be inferred by double scrambling tests or the triple scrambling

test

In Figure 1Ci, all objects exclude each other, except for a single event of perfect triple overlapping (white object in the center). Albeit low (MOC_{RGB}=0.0286), this triple overlapping cannot be taken as casual, as it would be interpreted if only taken into consideration double scrambling and triple scrambling tests (SE-SE-SE and NS, respectively) (Figure 1Cii). In this scenario, there are no yellow, magenta nor cyan pixels, all pixels involved in a pairwise overlapping are also involved in a triple one (Figure 1Ci). This colocalization is difficult to occur by chance, as single scrambling tests show all SC (Figure 1Cii). Conversely, Figure 1Ciii shows an image with randomly positioned overlapped pairs of objects. Yellow objects are actually R and G overlapped objects, magenta objects are R and B objects, and cyan objects are G and B objects. Casual overlapping of pairs of a different kind generates casual triple overlapping. Single scrambling tests (all NS) reveal the casual nature of this triple overlapping, contrasting to the triple scrambling test (SC) (Figure 1Civ). These examples show how the triple scrambling test fails to judge triple colocalization by overestimation (Figure 1Civand Fig. 1Biv) or underestimation (Figure 1Cii). In these examples, single scrambling tests are consistent with the real nature of images. For a triple overlapping deliberately generated (Figure 1Ci), the test yields SC even regarding the small MOC_{RGB} (0.0286) and opposite results of pairwise relationships (SE-SE-SE) (Figure 1Cii). On the other hand, when triple overlapping was generated by a random procedure (Figure 1Ciii), the test yields NS, even when MOC_{RGB} yields a higher value (0.1573) and pairwise relationships are all SC (Figure 1Civ). It's useful to mention that it is worthless to search the LRC in these examples, since pairwise relationships are almost symmetrical (similar p-values in double scrambling tests).

3.1.3 All scrambling tests contribute to interpret and classify different triple colocalization scenarios

To show the importance of a multitest approach, we made a colocalization analysis for all phases of the cell division. The complete cycle was taken from a single image downloaded from the library https://wellcomecollection .org/works/r8ppshar. Figure 2 shows the phases of the mitosis in raw merges (Figure 2A), binarized merges with regions of interest delimited (Figure 2B), and analytical results (Figure 2C), in which R represents kinetochores, G tubulin, and B DNA. As in the previous sections, in this biological model, the LRC test shows more consistent results with the nature of images and biological facts than the triple scrambling test. The LRC test (Figure 2C, highlighted in bold type) and triple scrambling test yielded different results in the interphase, early anaphase, and telophase (Figure 2C). In the interphase, tubulin (G) is restricted to the cytosol, and kinetochores (R) and DNA (B) are located in the nucleus. Although limitations on the resolution of images mainly generate a certain degree of triple overlapping, this is an exclusion scenario since the biomolecules are located in different compartments. The LRC test judges this relationship as SE, while the triple scrambling test yields NS. In early anaphase, kinetochores (R) and tubulin (G), which are mostly located at the poles of the cell, colocalize significantly. Chromosomes (B), whose ends are still centered, are overlapped with the other two channels in a degree comparable to random levels. This phase resembles the scenario of Figure 1B, with the same significance in all tests (Figure 1B and Figure 2C early anaphase). As in Figure 1B, in the early anaphase, the LRC (B) overlaps with the other two channels at a degree close to the mean of the random distribution of this channel. The LRC test (NS) allows to distinguish the triple relationship of the early anaphase to the one of the anaphases, in which chromosomes concluded their migration to the cell poles, and all single and triple tests yield SC. The LRC test also detects the disruption of the mitotic spindle in the telophase and the reorganization of the cytoskeleton towards the interphase. Although the LRC test allows better discrimination of the triple relationships of the mitosis phases, all statistical tests are useful for classifying all phases analytically. Prophase and telophase share the same results for double scrambling tests, and the LRC test. However, triple scrambling is NS in prophase and SC in telophase, evidencing that the general trend of triple overlapping is stronger than in prophase. Additionally, red scrambling is NS in prophase and SC in telophase, evidencing (in telophase) a significant trend of red signal to look for overlapped blue and green signals. Each scrambling test unveils a particular statistical fact, and from the synthesis of all of them, it is possible to classify all phases of mitosis analytically.

For reasons of convenience to show the results, the MOC coefficient was used for this work. Nevertheless, to overcome the controversy generated around this tool (Jeremy Adler & Parmryd, 2010, 2019), we performed all analyses for MCC coefficients too, obtaining equivalent results for all significances of all figures (Figure 3C)

3.2. Discussions

This work highlighted three important issues about triple colocalization analysis: **first**, the LRC test is a better test to judge significant triple colocalization than the triple scrambling test, which is the test performed by Fletcher (Fletcher *et al*., 2010). The LRC test evidences the exclusion existing in the interphase where interactors reside in different compartments. The LRC test also evidences the random nature of the configuration simulated in Figure 1Band reproduced in the early anaphase and the telophase. **Second**, triple colocalization cannot be inferred from pairwise relationships. This point is mainly evidenced by Figure 1C in which a triple SC can be found in a scenario where all pairwise relationships are SE; and adversely, a NS triple colocalization is yielded when all pairwise relationships are SC. **Third**, all scrambling tests are important to classify different scenarios. All phases of mitosis are distinguished by the result of at least one scrambling test, and each scrambling test is useful to contrast a specific statistical fact.

Although we restrict the study to 2D co-occurrence analysis, the concepts discussed in this work can be extrapolated to other branches of colocalization analysis, such as correlation approaches, object-based approaches, and coordinate-based analysis (Jaskolski, Mulle, & Manzoni, 2005; Malkusch *et al*., 2012), as well as other data features as 3D or super-resolution images.

4. CONCLUSIONS:

Identifying the channel that least colocalizes with the other two is the key to evaluating triple colocalization in cases of strong asymmetries of double relationships. In other scenarios, single scrambling tests can reveal significant triple colocalization for low levels of triple co-occurrence, even when all pairwise relationships were excluded. And, on the other hand, single scrambling tests can reveal the absence of a significant triple colocalization for high levels of triple co-occurrence, even when all pairwise relationships were significant colocalization. Furthermore, all scrambling test are useful for classifying a specific scenario of a triple relationship.

5. DECLARATIONS

5.1. Study Limitations

Besides the sample size, no other limitations were known at the time of the study.

5.2. Acknowledgements

We thank Thomas Surrey (Cancer Research UK, London, England), Oscar Bello (Yale School of Medicine New Haven, USA), and Luis Mayorga (IHEMCONICET, Mendoza, Argentina) for critically reading this manuscript.

5.3. Funding source

This work was supported by Foncyt PICT 2116, PIP-CONICET and SeCTyP grants to M. T. D.

5.5. Open Access

This article is licensed under a Creative Commons Attribution 4.0 (CC BY 4.0) International License, which permits use, sharing, adaptation, distribution, and reproduction in any medium or format, as long as you give appropriate credit to the original author(s) and the source, provide a link to the Creative Commons license, and indicate if changes were made. The images or other third-party material in this article are included in the article's Creative Commons license unless indicated otherwise in a credit line to the material. Suppose material is not included in the article's Creative Commons license, and your intended use is not permitted by statutory regulation or exceeds the permitted use. In that case, you will need to obtain permission directly from the copyright holder. To view a copy of this license, visit http://creativecommons.org/licenses/by/4.0/.

6. REFERENCES:

1. Aaron, J. S., Taylor, A. B., & Chew, T. L. (2018). Image colocalization - Co-occurrence versus correlation. *Journal of Cell Science*, *131*(3). https://doi.org/10.1242/JCS.211847
2. Adler, J., Pagakis, S. N., & Parmryd, I. (2008). Replicate-based noise corrected correlation for accurate measurements of colocalization. *Journal of Microscopy*, *230*(1), 121–133. https://doi.org/10.1111/j.1365-2818.2008.01967.x
3. Adler, Jeremy, & Parmryd, I. (2010). Quantifying colocalization by correlation: The pearson correlation coefficient is superior to the Mander's overlap coefficient. *Cytometry Part A*, *77*(8), 733–742. https://doi.org/10.1002/cyto.a.20896
4. Adler, Jeremy, & Parmryd, I. (2019). Quantifying colocalization: The MOC is a hybrid coefficient - An uninformative mix of co-occurrence and correlation. *Journal of Cell Science*, *132*(1), 1–3. https://doi.org/10.1242/JCS.222455
5. Bolte, S., & Cordelieres, F. P. (2006). A guided tour into subcellular colocalization analysis in light microscopy. *Journal of Microscopy*, *224*(December), 213–232.
6. Costes, S. V., Daelemans, D., Cho, E. H., Dobbin, Z., Pavlakis, G., & Lockett, S. (2004). Automatic and quantitative measurement of protein-protein colocalization in live cells. *Biophysical Journal*, *86*(6), 3993–4003. https://doi.org/10.1529/biophysj.103.038422
7. Dunn, K. W., Kamocka, M. M., & McDonald, J. H. (2011). A practical guide to evaluating colocalization in biological microscopy. *American Journal of Physiology - Cell Physiology*, *300*(4), 723–742. https://doi.org/10.1152/ajpcell.00462.2010
8. Fay, F. S., Taneja, K. L., Shenoy, S., Lifshitz, L., & Singer, R. H. (1997). Quantitative digital analysis of diffuse and concentrated nuclear distributions of nascent transcripts, SC35 and poly(A). *Experimental Cell Research*, *231*(1), 27–37. https://doi.org/10.1006/excr.1996.3460
9. Fletcher, P. A., Scriven, D. R. L., Schulson, M. N., & Moore, E. D. W. (2010). Multi-image colocalization and its statistical significance. *Biophysical Journal*, *99*(6), 1996–2005. https://doi.org/10.1016/j.bpj.2010.07.006
10. French, A. P., Mills, S., Swarup, R., Bennett, M. J., & Pridmore, T. P. (2008). Colocalization of fluorescent markers in confocal microscope images of plant cells. *Nature Protocols*, *3*(4), 619–628. https://doi.org/10.1038/nprot.2008.31
11. Goucher, D. R., Wincovitch, S. M., Garfield, S. H., Carbone, K. M., & Malik, T. H. (2005). A quantitative determination of multi-protein interactions by the analysis of confocal images using a pixel-by-pixel assessment algorithm. *Bioinformatics*, *21*(15), 3248–3254. https://doi.org/10.1093/bioinformatics/bti531
12. Jaskolski, F., Mulle, C., & Manzoni, O. J. (2005). An automated method to quantify and visualize colocalized fluorescent signals. *Journal of Neuroscience Methods*, *146*(1), 42–49. https://doi.org/10.1016/j.jneumeth.2005.01.012
13. Lachmanovich, E., Shvartsman, D. E., Malka, Y., Botvin, C., Henis, Y. I., & Weiss, A. M. (2003). Colocalization analysis of complex formation among membrane proteins by computerized fluorescence microscopy: Application to immunofluorescence co-patching studies. *Journal of Microscopy*, *212*(2), 122–131. https://doi.org/10.1046/j.1365-2818.2003.01239.x
14. Lagache, T., Sauvonnet, N., Danglot, L., & Olivo-Marin, J. C. (2015). Statistical analysis of molecule colocalization in bioimaging. *Cytometry Part A*, *87*(6), 568–579. https://doi.org/10.1002/cyto.a.22629
15. Li, Q., Lau, A., Morris, T. J., Guo, L., Fordyce, C. B., & Stanley, E. F. (2004). A Syntaxin 1, Gαo, and N-Type Calcium Channel Complex at a Presynaptic Nerve Terminal: Analysis by Quantitative Immunocolocalization. *Journal of Neuroscience*, *24*(16), 4070–4081. https://doi.org/10.1523/JNEUROSCI.0346-04.2004
16. Lifshitz, L. M. (1998). Determining Data Independence on a Digitized Membrane in Three Dimensions. *Image (Rochester, N.Y.)*, *17*(2), 299–303.
17. Malkusch, S., Endesfelder, U., Mondry, J., Gelléri, M., Verveer, P. J., & Heilemann, M. (2012). Coordinate-based colocalization analysis of single-molecule localization microscopy data. *Histochemistry and Cell Biology*, *137*(1), 1–10.

https://doi.org/10.1007/s00418-011-0880-5
18. Manders, E. M. M., Stap, J., Brakenhoff, G. J., Van Driel, R., & Aten, J. A. (1992). Dynamics of three-dimensional replication patterns during the S-phase, analysed by double labelling of DNA and confocal microscopy. *Journal of Cell Science*, *103*(3), 857–862. https://doi.org/10.1242/jcs.103.3.857
19. MANDERS, E. M. M., VERBEEK, F. J., & ATEN, J. A. (1993). Measurement of colocalization of objects in dual-colour confocal images. *Journal of Microscopy*. https://doi.org/10.1111/j.1365-2818.1993.tb03313.x
20. Mcdonald, J. H., & Dunn, K. W. (2013). Statistical tests for measures of colocalization in biological microscopy. *Journal of Microscopy*, *252*(3), 295–302. https://doi.org/10.1111/jmi.12093
21. Oheim, M., & Li, D. (2007). Quantitative Colocalisation Imaging: Concepts, Measurements, and Pitfalls, 117–155. https://doi.org/10.1007/978-3-540-71331-9_5
22. Pawley, J. (2000). The 39 steps: A cautionary tale of quantitative 3-D fluorescence microscopy. *BioTechniques*, *28*(5), 884–888. https://doi.org/10.2144/00285bt01
23. Ramírez, O., García, A., Rojas, R., Couve, A., & Härtel, S. (2010). Confined displacement algorithm determines true and random colocalization in fluorescence microscopy. *Journal of Microscopy*, *239*(3), 173–183. https://doi.org/10.1111/j.1365-2818.2010.03369.x
24. Van Steensel, B., Brink, M., Van der Meulen, K., Van Binnendijk, E. P., Wansink, D. G., De Jong, L., … Van Driel, R. (1995). Localization of the glucocorticoid receptor in discrete clusters in the cell nucleus. *Journal of Cell Science*, *108*(9), 3003–3011. https://doi.org/10.1242/jcs.108.9.3003
25. Wörz, S., Sander, P., Pfannmöller, M., Rieker, R. J., Joos, S., Mechtersheimer, G., … Rohr, K. (2010). 3D Geometry-based quantification of colocalizations in multichannel 3D microscopy images of human soft tissue tumors. *IEEE Transactions on Medical Imaging*, *29*(8), 1474–1484. https://doi.org/10.1109/TMI.2010.2049857
26. Zinchuk, V., & Zinchuk, O. (2008). Quantitative colocalization analysis of confocal fluorescence microscopy images. *Current Protocols in Cell Biology*, (SUPPL. 39), 1–16. https://doi.org/10.1002/0471143030.cb0419s39

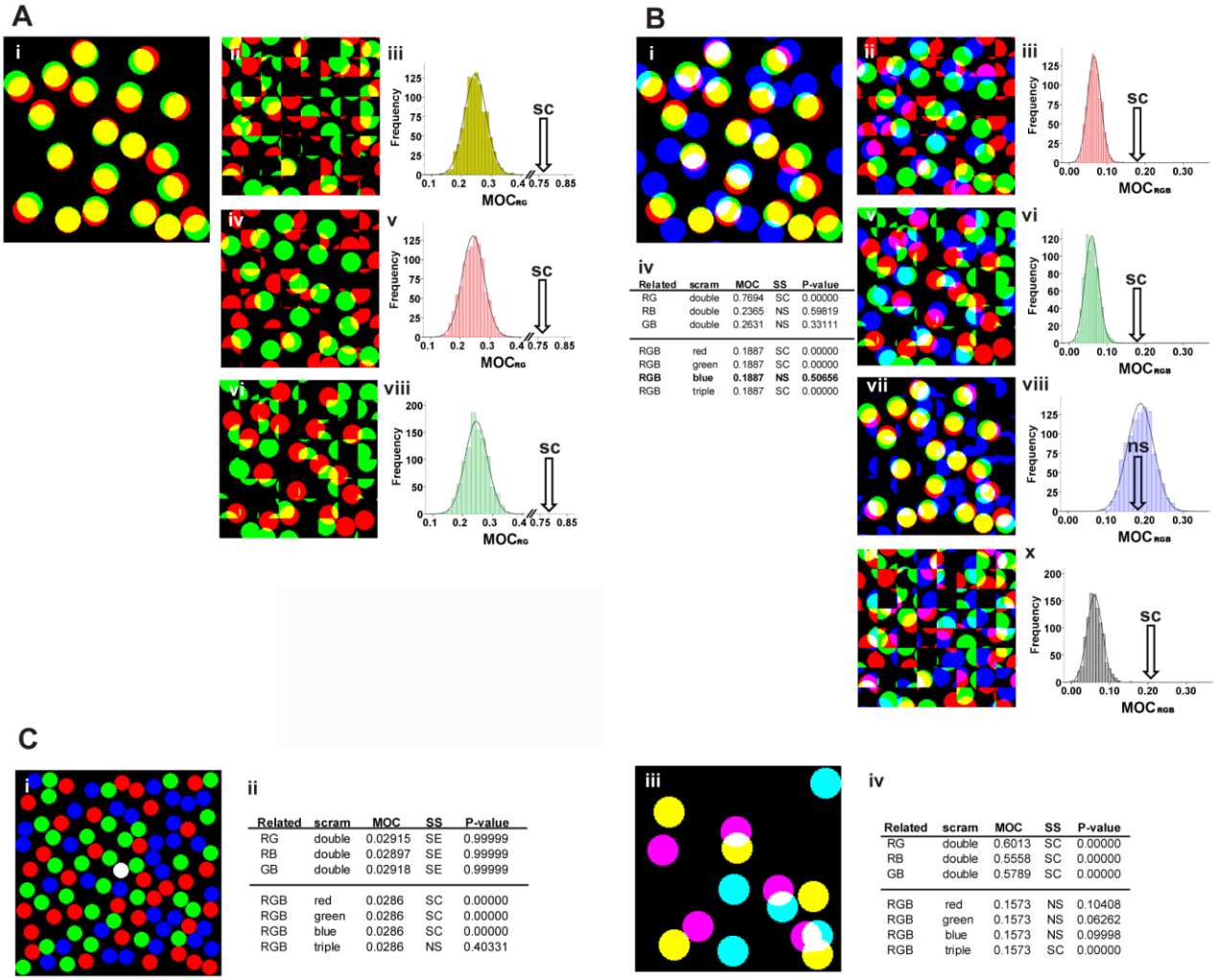

Figure 1: Different pairwise and triple colocalization scenarios. **A)** Left panel, two channels merge in a scenario of strong colocalization. Right panels, overlapping distribution of 1000 iterations of double, red, and green scrambling, actual overlapping value (arrow), and significance result. **B)** Left panels, three channels merge with the same red and green channels as in a) and a third blue channel with aleatory arranged objects; summary table showing the relationship analyzed, the channel/s scrambled, the MOC coefficient, the significance (SS) for an error of 0.05 and the p-value of significance calculated as the proportion of the area of the curve that is to the right of the actual overlapping value. The least related channel (LRC) (highlighted in bold type) is the channel that is not involved in the pairwise relationship with the smallest p-value. Middle panels include red, green, blue, and triple scrambling, respectively. Right panels, overlapping distribution of 1000 iterations of red, green, blue, and triple scrambling, actual overlapping value (arrow), and significance result. **C)** Left panels, the colocalization scenario of significant triple overlapping without significant pairwise colocalization and summary table. The right panel is the colocalization scenario of significant pairwise colocalization for the three relationships and not significant triple overlapping and summary table.

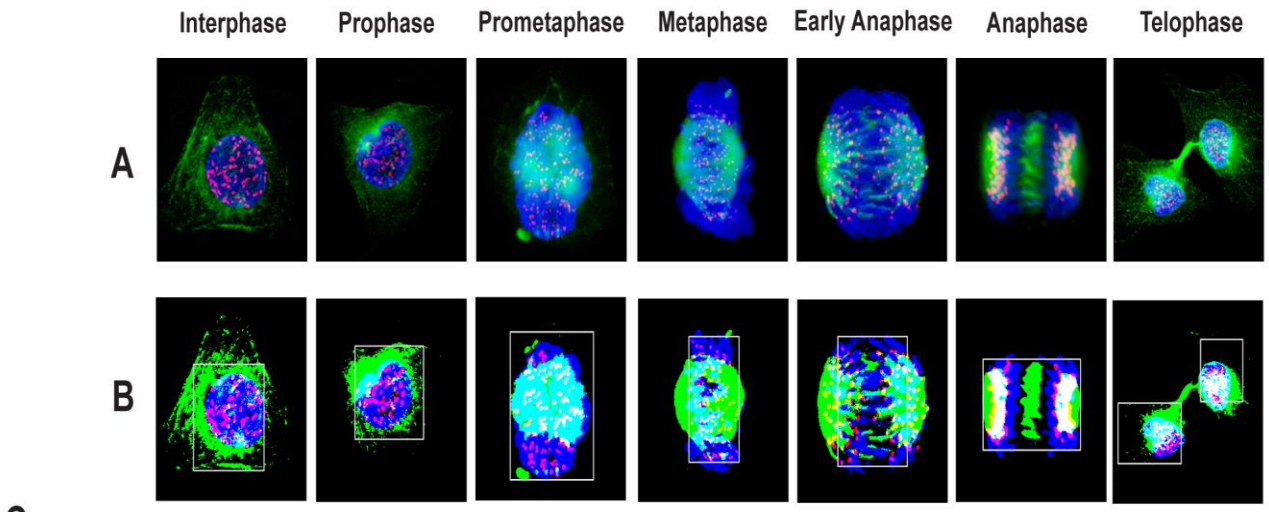

C

Related	Scram	MOC	SS	P-value	MOC	SS	P-value	MOC	SS	P-value	MOC	SS	P-value	MOC	SS	P-value	MOC	SS	P-value	MOC	SS	P-value
RG	double	0.09679	SE	0.99700	0.09314	NS	0.86400	0.335	SC	0.00000	0.3239	SC	0.03600	0.3473	SC	0.00000	0.6723	SC	0.00000	0.3644	NS	0.13500
RB	double	0.5452	SC	0.00000	0.4801	SC	0.00100	0.3888	SC	0.00000	0.3542	SC	0.04100	0.2491	NS	0.28300	0.6492	SC	0.00700	0.5871	SC	0.00000
GB	double	0.2075	SE	0.99900	0.3289	NS	0.58700	0.7512	SC	0.00600	0.4468	SE	1.00000	0.4524	NS	0.60000	0.4638	NS	0.58700	0.6412	NS	0.09100
RGB	red	0.07439	SC	0.00100	0.06224	NS	0.32100	0.2083	SC	0.00000	0.1452	SC	0.01300	0.1267	SC	0.00600	0.498	SC	0.00000	0.3014	SC	0.03800
RGB	green	**0.07439**	**SE**	**0.99900**	**0.06224**	**NS**	**0.84500**	**0.2083**	**SC**	**0.00200**	0.1452	NS	0.59600	0.1267	SC	0.01500	0.498	SC	0.00200	**0.3014**	**NS**	**0.15200**
RGB	blue	0.07439	SC	0.00000	0.06224	SC	0.02700	0.2083	SC	0.00500	**0.1452**	**NS**	**0.44800**	**0.1267**	**NS**	**0.45900**	**0.498**	**SC**	**0.02800**	0.3014	SC	0.00000
RGB	triple	0.07439	NS	0.47100	0.06224	NS	0.33700	0.2083	SC	0.00000	0.1452	NS	0.16600	0.1267	SC	0.01100	0.498	SC	0.00000	0.3014	SC	0.00900

Figure 2: Colocalization analysis of the phases of the mitosis. **A)** three channels merge of HeLa cells of all phases of the mitosis. Kinethochres in red, tubulin in green and DNA in blue. **B)** merges binarized at the same intensity thresholds used to calculate colocalization coefficients. Gray squares show the ROIs used for the analysis. **C)** Colocalization analysis for each phase showing: the MOC coefficient, the significance (SS) for an error of 0.05 and the P-value of significance. The LRC (highlighted in bold type) is the channel which is not involved in the pairwise relationship with the smallest p-value. MOC values were calculated for signal thresholds equal to the average intensity value of signal inside the ROI.

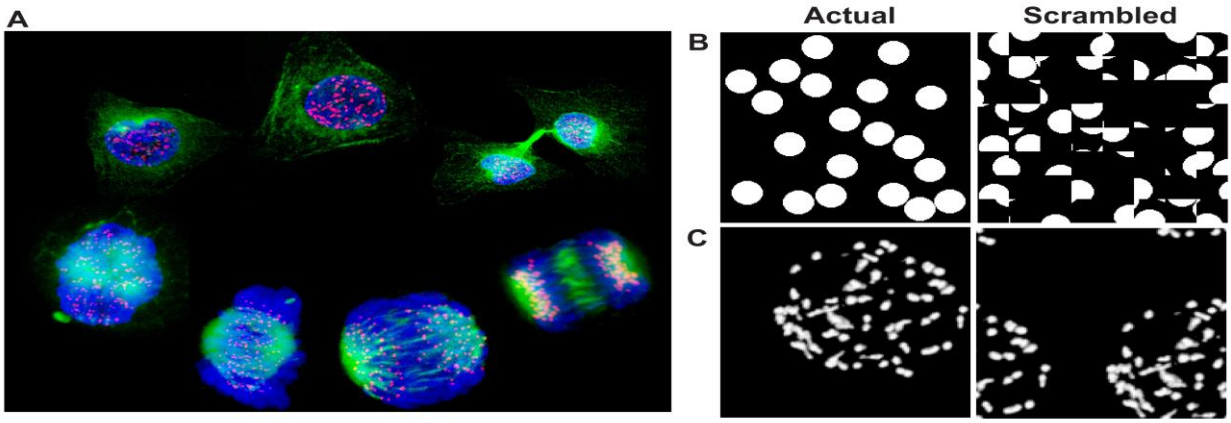

D

Related	Scram	MOC	SS	P-value	MCC	SS	P-value
RG	double	0.09679	SE	0.99700	0.242	SE	0.99800
GR	double				0.06599	SE	0.99900
RB	double	0.5452	SC	0.00000	0.9954	SC	0.00000
BR	double				0.3417	SC	0.00000
GB	double	0.2075	SE	0.99700	0.2223	SE	1.00000
BG	double				0.2645	SE	0.99800
R-GB	triple	0.07439	NS	0.37700	0.239	NS	0.30700
G-RB	triple				0.06426	NS	0.44900
B-RG	triple				0.08159	NS	0.26500
R-GB	red	0.07439	SC	0.00200	0.239	SC	0.00000
G-RB	green	0.07439	SE	0.99900	0.06426	SE	1.00000
B-RG	blue	0.07439	SC	0.00000	0.08159	SC	0.00000

Figure 3: Original cell cycle image, scrambling examples, and MCC results. **A)** Original image of the cell cycle. **B)** Example of Costes scrambling approach. The original image is in the left panel, and the scrambled image is in the right panel. **C)** Example of Lifshitz scrambling approach. The original image is in the left, and the scrambled images in the right. **D)** comparison of the results obtained for MOC and MCC in the interphase. Significances of MOC and MCC were equivalent for the rest of the phases (data not shown).